INVESTIGATION OF CLOUD PROPERTIES AND ATMOSPHERIC PROFILES WITH MODIS

SEMI-ANNUAL REPORT FOR JUL-DEC 1997

Paul Menzel, Steve Ackerman, Chris Moeller, Liam Gumley, Kathy Strabala,
Richard Frey, Elaine Prins, Dan LaPorte and Walter Wolf
CIMSS at the University of Wisconsin
Contract NAS5-31367

ABSTRACT

A major milestone was accomplished with the delivery of all five University of Wisconsin MODIS Level 2 science production software packages to the Science Data Support Team (SDST) for integration. These deliveries were the culmination of months of design and testing, with most of the work focused on tasks peripheral to the actual science contained in the code. UW hosted a MODIS infrared calibration workshop in September. Considerable progress has been made by MCST, with help from UW, in refining the calibration algorithm, and in identifying and characterization outstanding problems. Work continues on characterizing the effects of non-blackbody earth surfaces on atmospheric profile retrievals and modeling radiative transfer through cirrus clouds.

TASK OBJECTIVES

Software Development

Five UW science production software packages (cloud mask, cloud top properties, cloud phase, atmospheric profiles, and ancillary data) were delivered in fourth quarter 1997. The science portion of the algorithms have all been written and tested using MAS, AVHRR, HIRS and/or GOES data. Visualization tools for both MAS and MODIS data and products are being developed for testing and validation purposes.

MODIS Infrared Calibration

UW hosted a meeting of twenty scientists September 11 and 12 to discuss vacuum test results regarding the MODIS infrared calibration. The two day workshop concluded that the test data characterize the detector non-linearity and the cross-talk adequately so that the infrared calibration will be stable and within specification at launch. A final version of the infrared calibration algorithm will be achieved some months after MODIS launch in July 1998.

Algorithm Theoretical Basis Documents (ATBD's)

Two of the UW ATBD's (cloud mask, and cloud top properties and cloud phase) have been revised based upon the second ATBD panel reviews. They are now available electronically through the MODIS ATBD home page.

WORK ACCOMPLISHED

MODIS Software Development

A major milestone for 1997 was achieved with the successful delivery of the UW MODIS Version 2 algorithms. The algorithms included:

MOD_PR35 (Cloud Mask); delivered on 11/15/97,
MOD_PR07 (Atmospheric Profiles and ancillary data); delivered on 12/02/97,
MOD_PR06 (Infrared Cloud Height and Cloud Phase); delivered on 12/16/97.

These dates were in accordance with the delivery dates agreed upon at the October MODIS Science Team Meeting. The software delivery results from a major effort by the UW science algorithms development team of Liam Gumley, Rich Frey, Walt Wolf and Kathy Strabala. An outline of the this effort appears below.

1) An extraordinary amount of time and energy was spent in understanding and adhering to the toolkit requirements, coding standards, and metadata implementation.

2) A creation set of modules were written to automatically generate the product output file during execution based upon the original file specifications. This step insures that the output file and file specifications will match. This software is being used by all MODIS atmosphere group algorithm developers.

3) New routines for reading Level 1B data, geolocation data, and ancillary data were written to accommodate changing data formats.

4) Wrappers for metadata readers and writers, which were provided by the Science Data Support Team (SDST), were written and tested. This include ECS Core, Inventory, and Archive metadata.

5) Error handling, messaging and debugging strategies were designed and implemented in the Version 2 software.

6) A new ancillary data pre-processor was written. It consists of a GRIB decoder modified from code written by Neal Devine (which was modified from the program wgrib). It reads three GRIB encoded files from NCEP containing ancillary data needed by all atmosphere team software, and writes the data into 3 separate binary output files, meteorological data, ozone data, and ice concentration data. The GRIB decoder was written as a subroutine to be called from the main ancillary data routine. The files which are read and created are defined in the local pcf file, and accessed as temporary files in the main program.

7) Infrared Cloud Height and Cloud Phase algorithms were integrated into one mini-main subroutine as requested by Rich Hucek, SDST atmosphere group integration lead. The subroutine now returns parameters to the main program which will be used to insert metadata values for the complete MOD06 product.

8) All algorithms were successfully tested with 4 different simulated MODIS Level 1B input datasets including:

- Day over land/ocean,
- Day/night over South Pole,
- Day/night over terminator crossing,
- Night over ocean.

9) All delivered software complied with SDST FORTRAN-77 FORCHECK standards and SDST coding guidelines.

10) All coding runtime floating point exceptions (e.g. overflows, underflows, divides by zero) were eliminated.

11) Liam Gumley wrote IDL visualization software for both the simulated data and UW MODIS products specifically designed to aid in testing and development of the algorithms.

12) All production software was delivered and accepted by the SDST

13) Finally, the CIMSS MODIS group continues to work with SDST to ensure smooth transition of the UW MODIS algorithms into the PGS environment.

Level 3 Software

Walter Wolf continues to work with SDST to create the atmosphere group level 3 (MOD08) output HDF product file. This work includes making modifications to the CDL and to the existing C code, which reads in the file specification and creates an output FORTRAN subroutine containing all the information from the CDL file. This output FORTRAN subroutine is then used by SDST software to create the output level 3 HDF file automatically.

Visualization Software

An upgraded version of a visualization program for MAS data was released on the World Wide Web at http://cimss.ssec.wisc.edu/~gumley/sharp/sharp.html. It's main purpose is to aid in the development and testing of the UW MODIS production software packages. The program, developed by Liam Gumley and called SHARP, is a freely available IDL-based viewer for MAS image data that offers a point-and-click interface with the following features:

Selection of any scene (716x716 pixels) in a MAS HDF file,
View any spectral band for a scene (with title and color scale),
Automatic scaling to reflectance or brightness temperature,
Continuous display of data value under cursor,
Image creation via user defined band,
Enhance/stretch image with B&W or color lookup tables,
Scaling of image data into a specified range,
Interactive scatter plots with,
    User selected image regions (rectangle, circle, polygon),
    User selected X and Y axis band formulas,
    User selected X and Y axis limits,
    User selected regions (up to 10 regions with 10 different colors),
RGB image display,
Overlay of cloud mask results,
Overlay of HIS IFOV locations,
Projection onto a map base,
Immediate output to GIF or Postscript.

Figure 1 shows the SHARP display of a MAS image with a cloud mask overlay. This program was demonstrated at the HDF-EOS Developers Meeting, NASA/GSFC, 8-10 September, and at the MODIS Science Team Meeting, 22-24 October. It is expected to play an important role in validation and dissemination of the MAS cloud mask.

Web Based MODIS Visualization Tool

The UW MODIS team has worked in collaboration with UW McIDAS staff to develop visualization tools for MODIS. An initial version enables a modest subset of the McIDAS capabilities to view and investigate MODIS simulated data sets. UW assisted in the definition of the basic functions which would be needed by the MODIS science team. These include visualization of calibrated data, navigation (including maps), data fusion (overlays), and remapping to other satellite projections. These capabilities will be accessible through the web. This effort was funded by SDST to be used by the entire Science Team.

UW MODIS SCF

Planning for the at-launch UW MODIS Science Computer Facility (SCF) hardware began in earnest. The decision was made to stay with SGI hardware for compatibility with current systems at GSFC and UW. Silicon Graphics Origin2000 hardware was ordered for the CIMSS MODIS SCF. Components included were as follows:

    Origin2000 rack system with 2 x R10000 195MHz CPUs,
    512 MB RAM,
    Origin Vault RAID with 15 x 9GB disk drives.

This hardware will arrive at CIMSS in January 1998. Existing Origin2000 deskside CPUs within CIMSS will be integrated into the MODIS rack system to provide a single system with up to 16 CPUs that will be shared by MODIS and other CIMSS projects.

UW is investigating whether MODIS networking needs will be met by the NSF vBNS upgrade on the UW campus. By the time of MODIS launch there should be a good understanding of whether or not vBNS is capable of fulfilling our MODIS networking needs.

MODIS Infrared Calibration

UW hosted a meeting of twenty scientists September 11 and 12 to discuss vacuum test results regarding the MODIS infrared calibration. The two day workshop concluded that the test data characterize the detector non-linearity and the cross-talk adequately so that the infrared calibration will be stable and within specification at launch. However, much work remains to correct for the infrared cross-talk of the window channel into the carbon dioxide sensitive channels (more on this later in this report). It is expected that the inflight spacecraft roll to space will help to detail the scan mirror emissivity as a function of angle of incident radiation; this is necessary to determine the calibration blackbody emissivity. A final version of the infrared calibration algorithm will be achieved some months after MODIS launch in July 1998.

The MCST analysis was reviewed to determine the appropriate range of scene temperatures to be used in the calibration least squares fit; quadratic versus cubic fits were also studied. UW recommended that MCST extend the fitting range to include colder scene temperatures for bands 20-23, 29, 31 and 32. This will improve calibration of cold cloud scenes (temperatures less than 240K). UW also recommended that MCST apply a cubic fit to bands 20-23 in order to improve the fit at cold scene temperatures. However, care must be taken so that the accuracy of the calibration between 0.3 Ltyp and 0.9 Lmax is not be compromised. MCST has generated new calibration coefficients based on these recommendations and is proceeding with incorporating these recommendations into the MODIS Level 1B algorithm.

MAS Calibration

Monochromator measurements of the MAS IR spectral response functions (SRF) from February 1997 have been atmospherically and spectrally corrected for application to the MAS WINCE data set. Spectral corrections (+1.5nm for Port 3 and +7nm for Port 4) were found to be similar to previous MAS monochromator SRF measurements (within about 1% of MAS channel bandpass); this indicates consistent performance by the monochromator measuring system in the Ames Research Center (ARC) calibration facility. Comparison of February 1997 SRF to June 1996 SRF indicate that Port 3 has shifted about 25nm to shorter wavelengths (15% of typical Port 3 channel bandpass) and Port 4 has shifted about 20nm to shorter wavelengths (5% of typical Port 4 channel bandpass). The atmospherically and spectrally corrected SRF for Feb 97 have been provided to ARC

for inclusion in final MAS calibration of the WINCE data set. ARC will process MAS Ports 1 and 2 SRF. SRF atmospheric and spectral correction software as well as forward model transmittance files have been transferred from UW to ARC to facilitate the SRF analysis. A MAS fast transmittance model has also been generated at UW using the Feb 97 monochromator SRF; this model is applicable to MAS WINCE data set investigations. MAS and HIS radiances collected during WINCE have been compared to assess MAS calibration accuracy. Scenes over open water in Lake Huron from Feb. 8 1997 were used. The biases are provided in Table 1. Window band biases (42, 44-46) are less than 1°C; however atmospheric band 49 and 50 biases are larger and "out of family" with the window band biases. This result may be due to inaccuracies of the spectral response characterization of atmospheric bands (e.g. inaccurate atmospheric correction) in the monochromator measurements, or unexpected spectral shift of the MAS Port 4 grating sometime between the February 8 flight and the monochromator measurements (February 20). Both possibilities have been and continue to be the subject of scrutiny in MAS calibration investigations. For example, MAS-HIS comparisons from the SUCCESS field program (Spring 1996) did not indicate unexpected spectral shifting of the MAS gratings. Also, applying a uniform spectral shift to MAS Port 4 bands would cause reduction of bias for some atmospheric bands, while increasing bias for other atmospheric bands. This does not support an unexpected spectral shift of the MAS grating. However, this behavior cannot yet be ruled out.

Table 1. MAS-HIS comparisons using WINCE data. MAS spectral calibration based on monochromator characterization. Biases are small and uniform for window bands but are markedly higher for atmospheric bands, possibly due to inaccurate spectral characterization.

MAS CH	Wave-length (μm)	MAS AVG	MAS VAR	HIS AVG	HIS VAR	M/H COV	M/H BIAS	M/H RMS	CORRE LATIO N
30	3.72	273.61	.34	269.76	1.55	.21	3.85	4.03	293
31	3.88	272.36	.29	273.29	.66	.25	.93	1.15	574
32	4.04	269.85	.24	270.98	.37	.20	1.12	1.22	681
33	4.20	248.70	.17	249.27	.49	.06	.58	.93	202
34	4.36	227.09	.64	225.80	1.62	.04	1.29	1.96	038
35	4.51	253.38	4.40	254.74	.09	.01	1.36	2.52	019
36	4.67	269.20	.25	270.09	.21	.22	.90	.91	953
37	4.83	267.82	.23	268.61	.23	.21	.79	.82	915
38	4.98	269.91	.34	260.98	12.05	.20	8.93	9.58	101
42	8.51	272.23	.28	272.65	.27	.25	.42	.47	915
43	9.69	258.30	.13	257.96	.20	.12	.33	.44	761
44	10.49	273.81	.29	274.01	.29	.27	.20	.28	919
45	11.00	273.86	.29	273.99	.29	.27	.13	.22	919
46	11.98	273.49	.31	273.52	.30	.29	.03	.19	937
47	12.88	271.20	.27	271.24	.27	.25	.04	.20	928
48	13.27	262.13	.12	262.22	.14	.11	.09	.19	852
49	13.80	243.67	.03	242.29	.04	.01	1.38	1.39	.252
50	14.26	225.44	.07	223.74	.05	.00	1.70	1.73	.000

FTIR measurements of the MAS spectral response are also being evaluated in a research mode as a possible replacement for the traditional monochromator-based approach. The FTIR system has the advantages of comprehensive spectral coverage (400 - 4000 cm^{-1}) for each measurement, improved signal to noise compared to the monochromator system, and requires less time to collect the data . The comprehensive spectral coverage facilitates identification of out of band response in each spectral band while improved signal to noise improves definition of spectral absorption features. A set of spectral response measurements using the FTIR system were collected in Feb. 1997. These were atmospherically corrected and compared to the monochromator measurements. The FTIR and monochromator measurements yield symmetric, triangular SRF, which is expected in grating instruments. The monochromator and FTIR SRF show good agreement with only small spectral position changes (< 30nm, ~5% of bandpass). However, small spectral position changes are important in atmospheric bands. A preliminary comparison of MAS and HIS atmospheric band data (Feb 8, 1997 WINCE flight) shows that using FTIR SRF results in higher MAS-HIS calibration bias than when using monochromator SRF (e.g. 2.5°C versus 1.7°C for band 50). This result will continue to be a subject of investigation. The possible implications include unexpected spectral shift of the MAS grating position sometime between the dates of February 8 and the monochromator and FTIR measurements (which were taken a few days apart, but no MAS related activities occurred in that interim), erroneous measurement by the FTIR system, or inaccurate atmospheric and spectral correction of the FTIR measurements.

The MAS SUCCESS and WINCE data sets have been calibrated and processed into Level-1B radiances for distribution from the GSFC DAAC. A comparison of MAS radiances produced at UW and at the GSFC DAAC revealed no differences.

MAS quicklook images in the SUCCESS Data Archive are being updated to match the MAS SUCCESS data available from the GSFC DAAC. Updates were submitted in mid October for inclusion in a SUCCESS archive CD ROM to be available for distribution in 1998.

MAS Participation in CAMEX3

Possible MAS participation in the CAMEX3 field program (to be held in Aug/Sep 1998 from Patrick AFB, FL) has been discussed with NASA organizers. Substituting MAS for MAMS on the ER-2 for one to two weeks near the end of the experiment is being considered. CAMEX3 presents opportunities to monitor clouds (microphysics, heights, detection) in tropical systems with co-incident DC-8 in situ data collection. It also represents the first opportunity for MAS to underfly MODIS in the post-launch A&E phase (clear scenes). The ER-2 will be equipped with a dropsonde capability for characterizing the atmosphere below the aircraft. MAS will contribute quicklook imagery and nadir brightness temperatures for selected bands as well as derived cloud products from case studies of interest to the CAMEX3 archive. A final decision by NASA on MAS participation is forthcoming.

AVHRR Cloud Mask Validation Activities

In anticipation of future MODIS cloud mask verification efforts, a prototype methodology has been developed using the AVHRR cloud mask product. Three complete Global Area Coverage (GAC) orbits are processed every day in near-real time, using the previous day's Level 1B data as input. Daytime coverage includes the Amazon Basin, Eastern North America, the Saudi Arabian Peninsula and Western Europe.

Hourly surface observations from ten selected sites in North America (manned weather stations only) closest in time to the satellite measurements are collected and compared to the cloud mask output. In one approach, surface reports are compared to the cloud mask confidences of clear sky for the GAC pixels nearest the station locations. A second approach compares the surface reports with cloud mask results from a collection of pixels located within 100 km of the stations. Currently, only results from daytime data are compared, but we hope to expand to nighttime hours and also to other regions of the world in the near future.

Figure 2 shows a bivariate histogram of the single-pixel comparisons for the month of August, 1997. Weather station cloud coverage is plotted on the x-axis and clear sky confidences on the y-axis. Taller columns indicate a higher frequency of occurrence. The cloud mask is generally doing a satisfactory job, particularly in the case of reported clear skies. This reflects the concern that the cloud mask should be conservative in designating pixels as "clear". Frequencies of confidences associated with the "few", "scattered", "broken", and "overcast" categories change as one would expect, as the likelihood of having clouds directly overhead increases with increasing cloud cover. Sky coverage for these categories is 1-2/8, 3-4/8, 5-7/8, and 8/8, respectively. A similar plot may be constructed showing the results of the second method, where the "percent of nearby pixels with confidence > 99%" replaces the "confidence of clear sky" on the y-axis. This plot (not shown) for the month of August 1997 displays a very similar distribution of frequencies.

A World Wide Web site has been constructed which shows results of the near-real time AVHRR cloud mask over North America. The site is updated daily and displays images of visible and IR radiance data along with cloud mask and land/sea tag information from the previous day's NOAA-14 overpass. Verification results are also shown. The site address is http://oldthunder.ssec.wisc.edu/poes/cldmsk.html

MAS Cloud Mask

Work has continued on a cloud mask algorithm which uses radiance data from the MODIS Airborne Simulator (MAS) instrument. An indication of thin cirrus cloud determined by use of solar and IR data (separately) has been added to the output which will also be included in the MODIS algorithm

Effects of Infrared Surface Emissivity

Visiting scientist Dr. Youri Plokhenko continues his investigation of MAS temperature/moisture retrieval sensitivity to surface emissivity. The approach of the study is to use a physical retrieval algorithm to determine atmospheric temperature/moisture and surface emissivity. Surface emissivity patterns determined for the SUCCESS data set have been correlated with NDVI patterns estimated with the MAS data; good correlations are found. This study has been expanded beyond the springtime SUCCESS data set over Oklahoma to include a wintertime WINCE data set over Lake Michigan. In the winter scenes of frozen tundra, surface emissivity effects were still significant. An example of this work is provided in Figure 3.

Radiative Transfer Through Cirrus Clouds

Dr. Sunggi Chung has been calculating the cloud forcing expected from various cirrus cloud formations. Using line by line code (LBLRTM) in combination with a discrete ordinate model (DISORT), ice particles of various sizes, water paths, and heights have been inserted into a clear sky atmosphere to investigate the spectral characteristics of the cloud forcing. Figure 4a shows the spectral cloud forcing from a 0.8 km layer of small ice particles (radius of 5 microns); Figure 4b shows the same for larger ice particles (radius of 12.5 microns). The linear versus nonlinear behavior of the cloud forcing in the infrared window between 750 and 1000 wavenumbers is being studied further.

DATA ANALYSIS

MODIS Infrared Calibration

(1) Optical crosstalk from MODIS band 31 into PC bands 32-36 is under investigation. Of interest are the spatial position of the crosstalk, the spectral characteristic of the "leaked" radiance, and the amplitude of the leaked radiance (with respect to band 31 radiance). The goal is to identify a correction algorithm that removes the out of band radiance from MODIS level 1B radiances.

Significant understanding of the spatial and spectral component and the direction of the crosstalk has been gained through the use of IAC data sets; across track or scan direction crosstalk (e.g. channel 5 of band 31 leaking into channel 5 of bands 32-36) is found to be one-way only, originating as a reflection at a position near the edge of the band 31 focal plane. This position is identified as the origin of crosstalk for all affected PC bands. The leaked radiance passes through the band 31 filter before being reflected to the other PC bands. It is difficult to uniquely identify along track crosstalk (e.g. channel 3 band 31 talking to channel 5 bands 32-36) in the IAC data sets. Some evidence that along track crosstalk exists has been found, however this is not conclusive; analysis is still under way to separate the test equipment and instrument contributions. Characterizing the spatial component of the scan direction crosstalk is difficult because the out of band radiance originates from parts of two adjacent band 31 fields of view. Methods to address this in a

crosstalk correction algorithm are under review. For a single field of view correction, an average of adjacent band 31 pixels is under consideration. A multiple field of view correction approach is also under consideration; this approach would correct the crosstalk into PC bands over NxN (TBD, 5x5 being considered) fields of view, reducing the sensitivity of the correction to the spatial characteristic.

A radiative transfer based investigation to assess the amplitude of the crosstalk into each PC band is underway. Radiometric data sets (RC-02) collected in T/V are being used. In this investigation, crosstalk is accounted for during the view of each source (SVS, OBC, BCS) and the crosstalk amplitude is formulated as a function of the band 31 inband radiance only. Importantly, this approach does not depend on the scene radiance of the xtalk-affected band. A simple linear model is applied:

$$L'_{i,j} = L_{i,j} + L_{31,j} * xtalk_{31,j \rightarrow i,j} * \left(\frac{resp_{i,j}}{resp_{31,j}} \right) \qquad (1)$$

where $L'_{i,j}$ is a target's digital count calibrated to a radiance for band i, channel j
$L_{i,j}$ is the measured radiance of a target for band i, channel j
$L_{31,j}$ is the measured radiance of a target for band 31, channel j
$xtalk_{31,j \rightarrow i,j}$ is the crosstalk amplitude from band 31, channel j into band i, channel j
$resp_{i,j}$ are the responsivities (L/dn) of bands i, channel j.

A 2nd order calibration based on MCST efforts is being applied in the retrieval.

$$L'_{i,j} = a_2 * dn_{i,j}^2 + a_1 * dn_{i,j} + a_0 \qquad (2)$$

where dn is digital number and the a values are calibration coefficients.

For the analysis, all crosstalk is assumed to be uni-directional across-track only (i.e. channel 5 of band 31 talks to channel 5 of bands 32-36 only); no along track crosstalk is allowed (e.g. channel 3 of band 31 talking to channel 5 of bands 32-36). Adjustments of the BCS, OBC, and SVS radiance for emissivity (based on SBRS/MCST analysis) and scan mirror reflectance (based on Lincoln Lab witness samples) were applied. Crosstalk amplitudes have been retrieved using the cold (UAID1315-1337), nominal (UAID1506-1526, UAID1595-1617) and hot (UAID1402-1426) plateau RC-02 data sets. The radiative transfer of the nominal data sets is more accommodating because the OBC, scan mirror and scan cavity are all at ambient temperature, reducing sensitivity to OBC emissivity and scan mirror reflectance uncertainty in the crosstalk amplitude retrieval. Retrieval results show a level of consistency between the nominal data sets, but the cold and hot plateau results are out of family (Figure 5) The nominal data set retrievals show

that band 36 is most affected, with bands 35, 34, and 33 showing progressively smaller leaks. The most reliable assessments of crosstalk amplitude are attained when BCS temperatures are high (> 300K in Figure 5); the radiance leak is large at warm BCS temperatures, thus making it easier to distinguish from background. It is important in the analysis that the crosstalk amplitude be independent of scene temperature (horizontal line for each band in Figure 5). This characteristic is best exhibited by the nominal data sets; however, it is noteworthy that an adjustment of the 2nd order calibration coefficient was required to reduce dependency on scene temperature. The implication of this is that the PC band 2nd order calibration coefficients may be contaminated by crosstalk. The crosstalk amplitude will continue to be analyzed. Inconsistency between the cold, hot and nominal data sets is currently not well understood; however, the more complex radiative transfer (large temperature contrast between instrument and components) of the cold plateau data set and the elevated background of the hot plateau data set are unlikely conditions of MODIS on-orbit performance and as such are lower priority data sets in the crosstalk investigation. UW and MCST are proceeding with the implementation of the linear correction approach in the MODIS Level 1B Radiance product code. The nominal data set results indicate that the linear approach is suitable.

(2) The wavelength correction of MODIS IR band RSR data has been discussed with and implemented by MCST. An analysis of central wavelength (CWL) as a function of position on the focal plane indicates a characteristic parabolic shape to the adjustment. Some selective editing to remove out of family CWL (especially at each end of the focal plane, i.e. channels 1 and 10) was applied to improve the fit of the model to the data. The average CWL from the parabolic curve will be used to define the wavelength correction for each channel. This procedure will be applied uniformly to all MODIS IR bands. Corrections were typically in the 0 to 10 nm range. The largest corrections (up to 10nm to shorter wavelengths in the LWIR) were made to channels 1 and 10, which reside at each end of the focal plane; channels in the middle of the focal plane (4-7) were corrected typically by 5nm or less to longer wavelengths while channels going towards the end of the focal plane (2,3,8,9) had the smallest corrections. On average, the wavelength corrections in the MWIR were 25 to 50% of those made in the LWIR. A few bands were considerably "out of family" with the parabolic model, most notably band 31. In this case, the parabolic model was applied to a highly subsampled group of CWL. The wavelength corrections translate to calibrated temperature adjustments of ~0.05K (window bands) to ~0.25K (atmospheric bands).

(3) A simulated one year global data set has been generated using forward calculations on radiosonde data with MAS and MODIS spectral response. The data set will be used initially to investigate a correction algorithm for 5.3um leakage into MODIS SWIR bands. It will also be useful for simulating MODIS performance in various parts of the globe, especially as benefits MODIS science algorithms.

CO_2-Slicing Cloud Height Algorithm Development

The effort to apply the CO_2-slicing cloud height algorithm to MAS data is continuing. Important details concerning the implementation of the algorithm in the MODIS processing environment will be made based on the results of tests conducted with MAS data. Questions remain relating to channel combination selection, spatial scale of retrievals (number of pixels from which to gather radiance data), surface temperature variations, and emissivity differences between channels.

Figure 6 shows imagery based on data taken from an ER-2 flight segment on April 26, 1996 during the SUCCESS field experiment. The left-most image shows 11 micron brightness temperatures (MAS band 45), while the other two depict cloud height retrievals using the CO_2-slicing method. The IR image shows an area of relatively thick (but still transmissive) cirrus surrounded by somewhat thinner cloud; some of it extremely thin. The rest of the scene is clear. The center image shows the results of the cloud height algorithm where clear-sky radiances have been calculated from nearby temperature and moisture profile measurements. The image on the right is the same except the "clear-sky" radiances are based on a sample of the ten warmest values from within a ten by ten pixel area. In both methods, cloudy radiances are based on a sample of the ten coldest values from the original 100. The magenta color corresponds to cloud heights of 100 mb, blue is 100-200 mb, and yellow is 200-300 mb with other colors representing still lower heights.

There are problems associated with both methods. The calculated clear radiance result is much more consistent over the region, but the cloud height retrievals over the thinnest clouds are too high (100 mb) according to lidar data which indicated clouds near 200 mb. Also, heights increase with distance from the thicker parts of the cloud, counter to most observations of cirrus clouds, and also not consistent with previous experience. On the other hand, the result shown on the right (using the ten warmest values in the gradient method) is very noisy, with many cloud height retrievals too low. However, both methods are more accurate than the simple "window" cloud height (not shown) where heights are too low everywhere in the image, except for the very thickest parts of the cloud.

Version 2 delivery of the MODIS CO_2-slicing algorithm included several modifications and enhancements. In order to indicate cloud top heights at greater vertical resolution, input atmospheric profiles of pressure, temperature, and transmittance are interpolated between original pressure levels from 670 mb to 200 mb. This increases the total number of pressure levels from 40 to 50 and enables cloud top pressure altitudes to be reported at approximately 25 mb intervals. Also included in the delivered software is an option allowing the algorithm to be run in three different modes. The first mode uses clear-sky radiances calculated from the nearest atmospheric temperature and moisture profiles to compare with observed radiances when computing cloud heights. The second mode uses cloud mask information to ascertain which pixels are clear and then develops mean clear-sky radiances for use in cloud height generation. The third method uses differences between the warmest and coldest radiances in a region (gradient method) and does not require a clear-sky radiance. The algorithm will use the first method for Day 1 processing.

Software was created for the purpose of generating cloud heights using MAS radiance data from HDF-format files as input. This will enable cloud heights to be generated quickly from the large archive of MAS data now available. The software will be used to further characterize and improve the MODIS cloud height algorithm.

GOES Biomass Burning Program

The following work is being funded under separate NASA (NAGW-3804) and NOAA contracts. It has relevance to the MODIS biomass burning studies.

GOES-8 ABBA and ASADA Results for the 1995 Fire Season in South America:

Over the past two years the GOES-8 Automated Biomass Burning Algorithm (ABBA) and the Automated Smoke and Aerosol Detection Algorithm (ASADA) have matured based on input from the SCAR-C and SCAR-B field programs. Multispectral GOES-8 data collected during the 1995 fire season (June-October) were reprocessed with the updated GOES-8 ABBA (version 5.5) and ASADA (version 3.0).

Diurnal GOES-8 ABBA results for 1995 (at 1145, 1445, 1745 and 2045 UTC) demonstrate the need for geostationary fire monitoring in the tropics. Although peak burning usually occurs in the middle of the afternoon local time, fires are lit throughout the day with flaming conditions only lasting for a short time. Daily totals of unique fire pixels observed at all 4 time periods with the GOES ABBA were typically 65% greater than the values at 1745 UTC. Only 20% of the fire pixels were detected in more than one time period. Nearly 340,000 fire pixels were detected with the GOES-8 ABBA from June through October 1995 with an estimated total burned area of approximately 42,000 km^2. Roughly 40% of the burning occurred during the SCAR-B field program with approximately 3,500 unique fire pixels detected per day from 15 August to 15 September. Most of the burning was concentrated along the perimeter of the Amazon. Many fires were also detected in Bolivia, Paraguay, and Northern Argentina. A fire composite (see Figure 7) for the entire season shows distinct burning patterns along rivers and in areas with recent road construction and associated settlements within Amazonia. The spatial distribution of fires depicted in this composite shows patterns and details similar to those identified by Skole and Tucker (Science, 1993) in their analysis of deforestation observed in Landsat imagery. On average, 35% (14,646 km^2) of the fire pixels were located in the broadleaf tropical forests; over 45% were located in the cerrado, shrub and grasslands (18,830 km^2).

Daily GOES-8 ASADA results (based on 1145 UTC GOES-8 imagery) for June through October 1995 show a sharp increase in smoke/aerosol coverage and intensity corresponding to peak burning in August and September and the first two weeks in October (see Figure 8). During the months of June and July the average smoke/aerosol coverage extended over 1.5 million km^2. In August and September the average size of the smoke pall was on the order of 4.5 million km^2. At the peak of the burning season the

GOES-8 ASADA detected a smoke pall extending over 7.9 million km^2 with derived smoke albedos 3 to 4 times higher than what was observed under clear conditions. The day to day variability in smoke coverage and intensity was directly linked to the amount of fire activity in the region.

The GOES-8 ABBA and ASADA results for each day of the 1995 fire season are now available via anonymous ftp at smokey.ssec.wisc.edu in the subdirectory pub/abba1995. The README file includes a description of the ASCII data files and GIF files contained in this directory. The GOES-8 fire and smoke products for SCAR-B and the 1995 season provide a benchmark in ongoing efforts to determine interannual trends in South American biomass burning from a geostationary platform from 1995 into the next century.

PAPERS

Ackerman, S. A., K. I. Strabala, W. P. Menzel, R. A. Frey, C. C. Moeller and L. E. Gumley, 1997: Discriminating Clear-sky from Clouds with MODIS. Submitted to the J. Geo. Res

Ackerman, S. A., S. Pryzbylak, K. T. Kriebel and H. Mannstein, 1995: A comparison of cloud water content derived from satellite retrieval techniques and surface observations. Submitted to Remote Sensing Environment.

Ackerman, S. A., C. C. Moeller, K. I. Strabala, H. E. Gerber, L. E. Gumley, W. P. Menzel, S-C. Tsay, 1997: Retrieval of effective microphyscial properties of clouds: a wave cloud case study, Accepted for publication in JGR Lett.

Moeller, C. C., D. D. LaPorte, K. I. Strabala, P. Hajek, and W. P. Menzel, Spectral characterization of MODIS Airborne Simulator (MAS) LWIR bands and application to MODIS science data cloud products. Earth Observing Systems II Conference, July 28-29, 1997, SPIE, pp 235-243.

King, M., S-C Tsay and S. A Ackerman, 1997: MODIS Airborne Simulator: Radiative properties of smoke and clouds during ARMCAS and SCAR-B, Third International Airborne Remote Sensing Conference and Exhibition, 7-10 July, Copenhagen, Denmark.

King, M. D., S.-C. Tsay, S. A. Ackerman and N. F. Larsen, 1997: Discriminating Heavy Aerosol, Clouds, and Fires During SCAR-B: Application of Airborne Multispectral MAS Data,. Submitted to J. Geo. Res.

Prins, E., J. Feltz, W.P. Menzel, and D. Ward, 1997: An overview of GOES-8 diurnal fire and smoke results for SCAR-B and the 1995 fire season in South America. Submitted to the Jour. of Geo. Res. Atmos., SCAR-B special issue.

Riggs, G. A., D. K. Hall , S. A. Ackerman Sea Ice Detection with the Moderate Resolution Imaging Spectroradiometer Airborne Simulator (MAS), 1997: Submitted to Remote Sensing Environ.

Smith, W. L., S. A. Ackerman, H. Revercomb, H. Huang, D. H. DeSlover, W. Feltz, L. Gumley and A. Collard, 1997: Infrared spectral absorption of nearly invisible cirrus clouds. Accepted for publication in JGR Lett.

Strabala, K. I., S. A. Ackerman, C. C. Moeller, L. E. Gumley, R. A. Frey, J. Y. Li and W. P. Menzel, 1996: Cloud Properties Determined from MODIS Airborne Simulator (MAS) SUCCESS Observations. Poster presented at the ERIM Third International Airborne Remote Sensing Conference and Exhibition held in Copenhagen, Denmark July 7-10, 1997.

MEETINGS

Kathy Strabala attended the ERIM Third International Airborne Remote Sensing Conference and Exhibition held in Copenhagen, Denmark July 7-10, 1997.

Chris Moeller presented a paper on MAS spectral calibration stability at the Second EOS conference of the SPIE 97 annual meeting on July 28-29, 1997.

E. Prins attended the Interagency Workshop on Requirements for Measuring/Monitoring Fires From Space at NASA Langley Research Center in Hampton, VA on September 4 and 5, 1998. She presented an overview of recent developments in diurnal remote sensing of fires using geostationary satellite multispectral imagery.

Paul Menzel, Chris Moeller, Dan LaPorte and Steve Ackerman attended the MODIS IR Calibration Workshop held in Madison, WI, on 11-12 September.

Liam Gumley attended the HDF-EOS Developers Meeting, NASA/GSFC, September 8-10.

Chris Moeller and Dan LaPorte met with Tom Pagano and Jim Young at SBRS, Santa Barbara, CA to discuss MODIS PC band crosstalk characterization and correction, October 9.

Paul Menzel, Steve Ackerman, Chris Moeller, Dan LaPorte, Liam Gumley, Kathy Strabala, Richard Frey and Walter Wolf attended the MODIS Science Team Meeting in College Park, Maryland, 22-24 October.

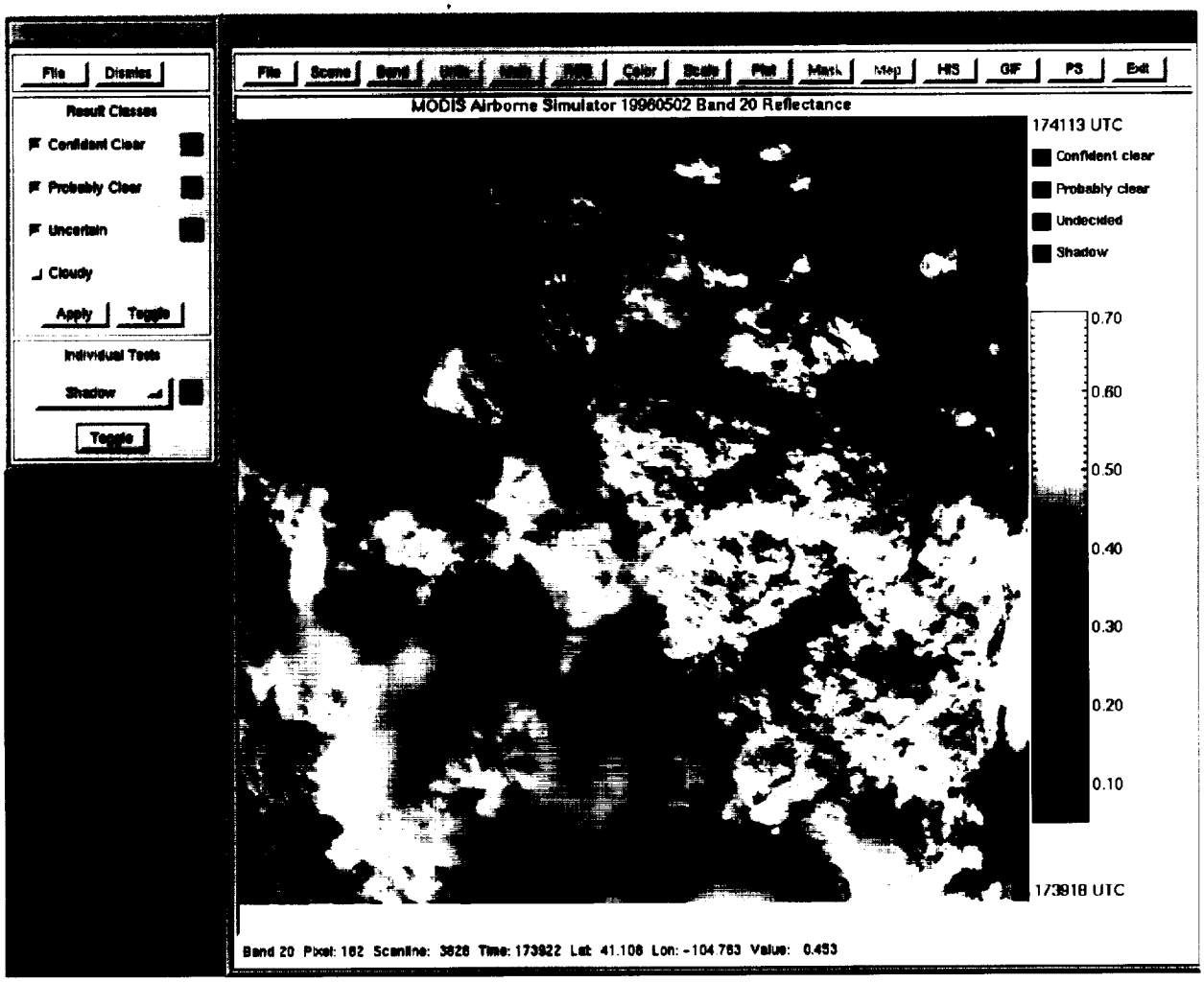

Figure 1. Screenshot from SHARP showing Cloud Mask Overlay.

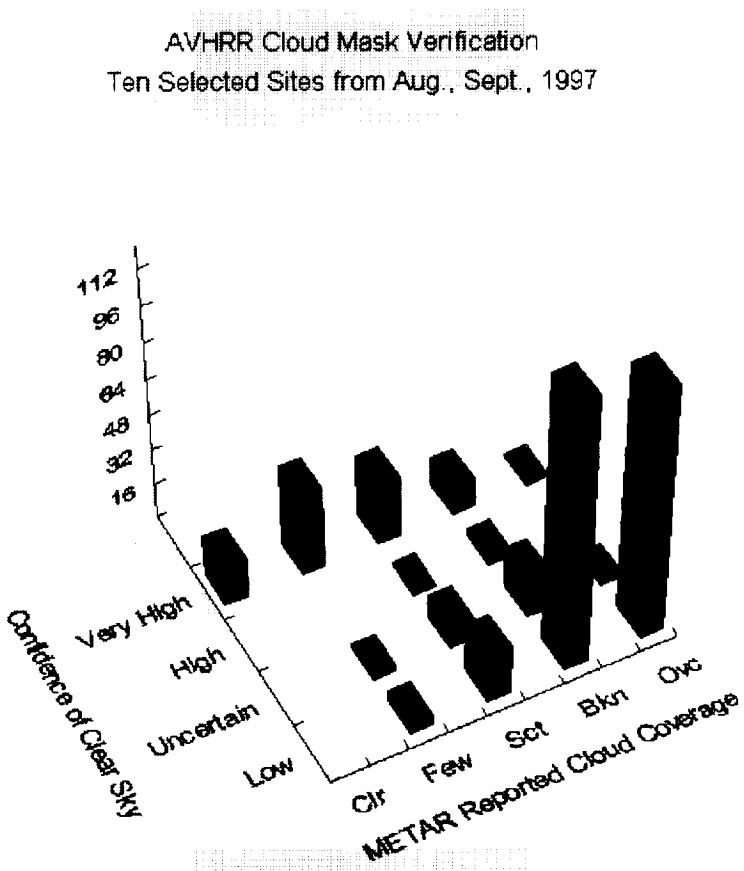

Figure 2. Results of comparison of automated AVHRR LAC cloud mask with ground station observations. Most points occur along the diagonal, which indicates agreement.

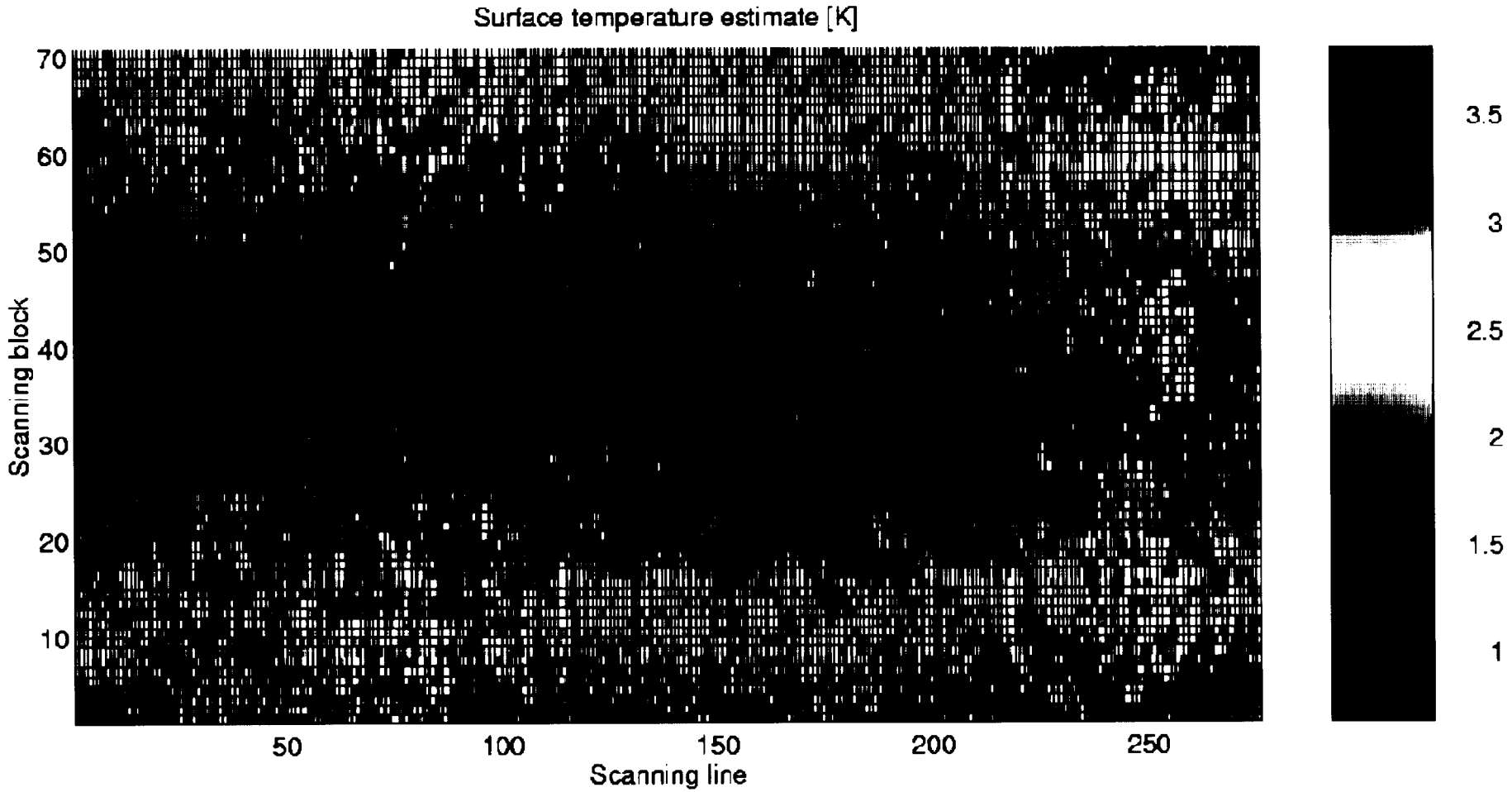

Figure 3. Difference of the surface temperature retrieval with and without reflection, derived from a 13 April 1996 SUCCESS MAS flight over the Cloud and Radiation Testbed (CART) site in Oklahoma. The data was averaged in 10 x 10 FOV's to reduce noise.

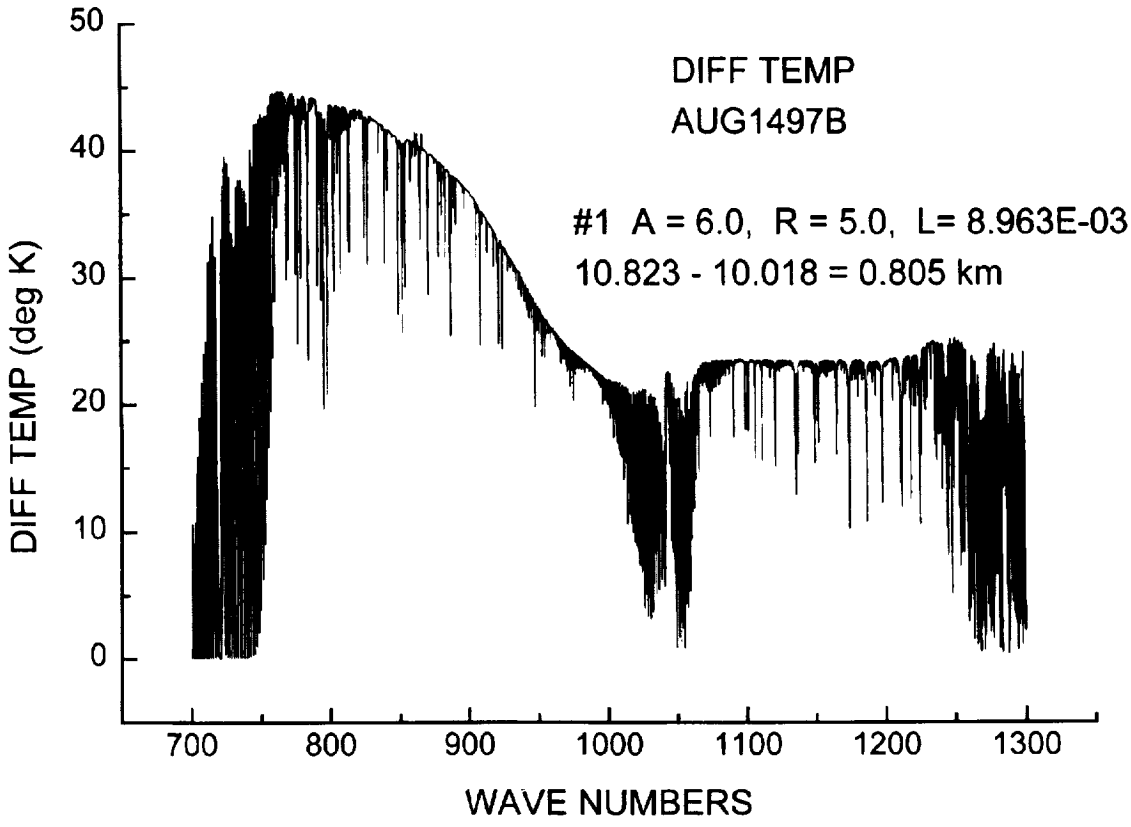

Figure 4a. Spectral Cloud forcing from a 10 km high 0.8 km thick layer of 5 micron ice particles.

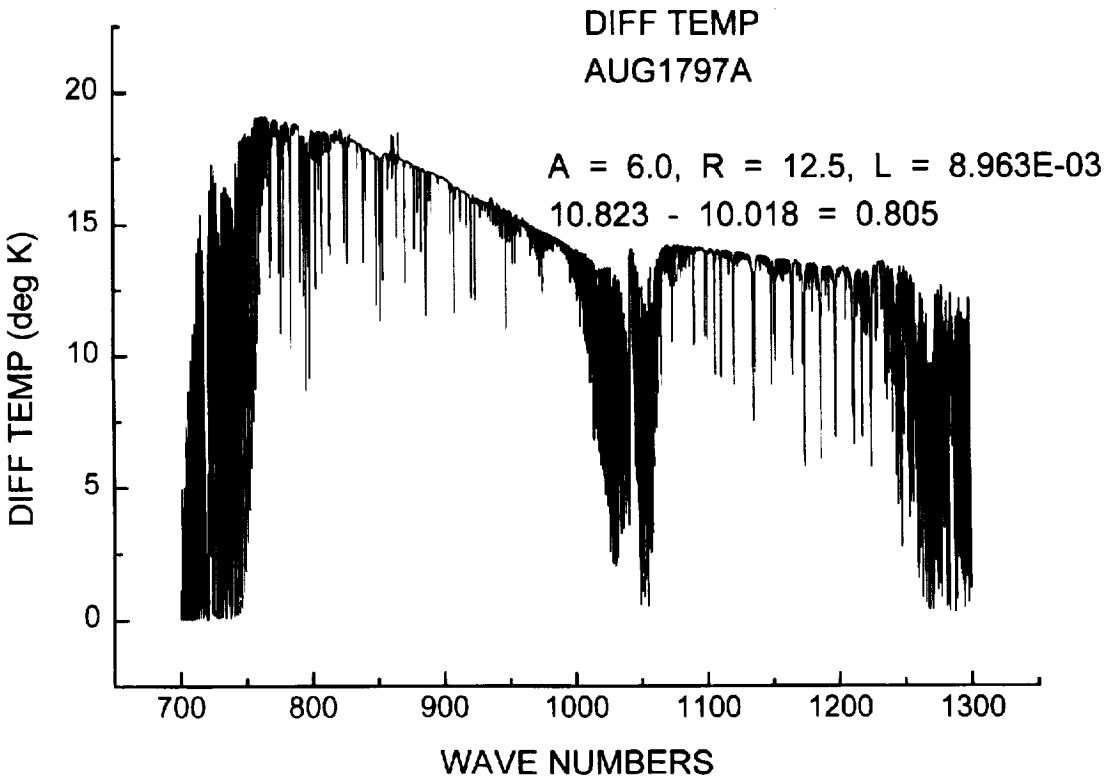

Figure 4b. Spectral Cloud forcing from a 10 km high 0.8 km thick layer of 12. 5 micron ice particles.

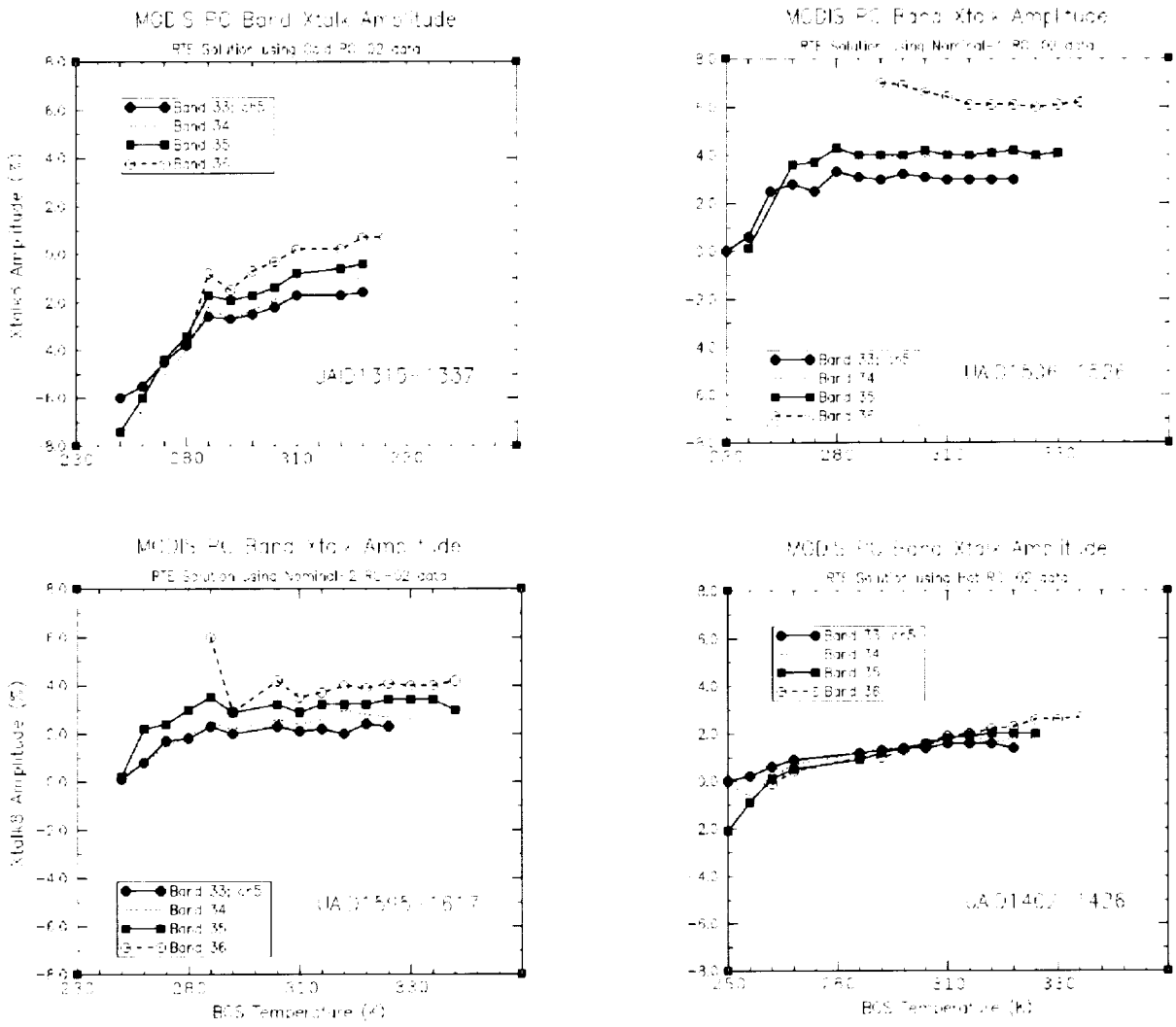

Figure 5. Crosstalk amplitude analysis for MODIS PC bands using cold (UAID1315-1337), nominal (UAID1506-1526, UAID1595-1617) and hot (UAID1402-1426) plateau data sets. Results are most meaningful for high BCS temperatures (>300 K). Results that show crosstalk amplitude is independent of scene temperature (i.e. horizontal trace with BCS temperature) are desired; this is attained in the nominal 1 and 2 data sets when adjusting the a coefficient in the 2nd order MODIS calibration.. Cold and hot plateau results are out of family with nominal data set results. Nominal data sets are the closest approximation to expected MODIS on-orbit performance.

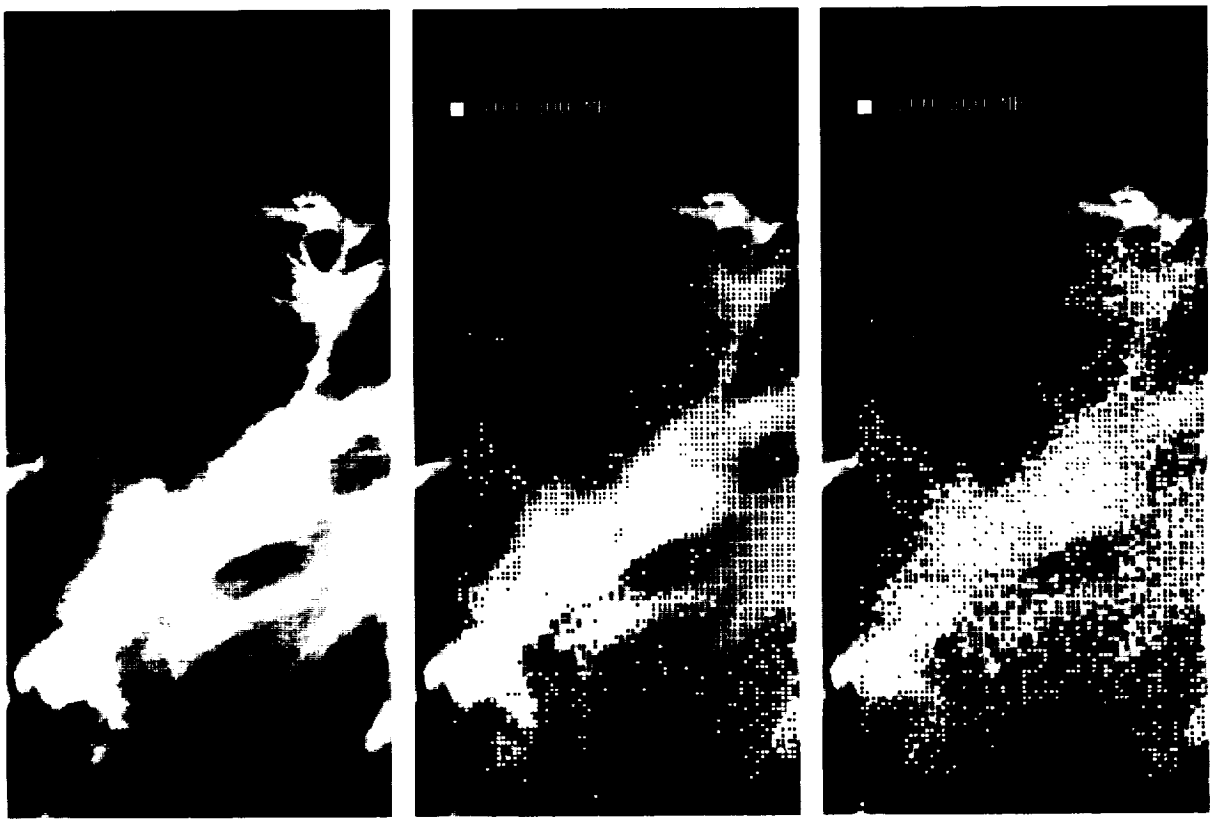

From left to right: MAS band 45, cloud heights using calculated clear radiances, and cloud heights using the gradient method

Figure 6. Results of two versions of the CO2 slicing cloud top height technique applied to a thin cirrus scene from the 26 April 1996 SUCCESS field experiment data set.

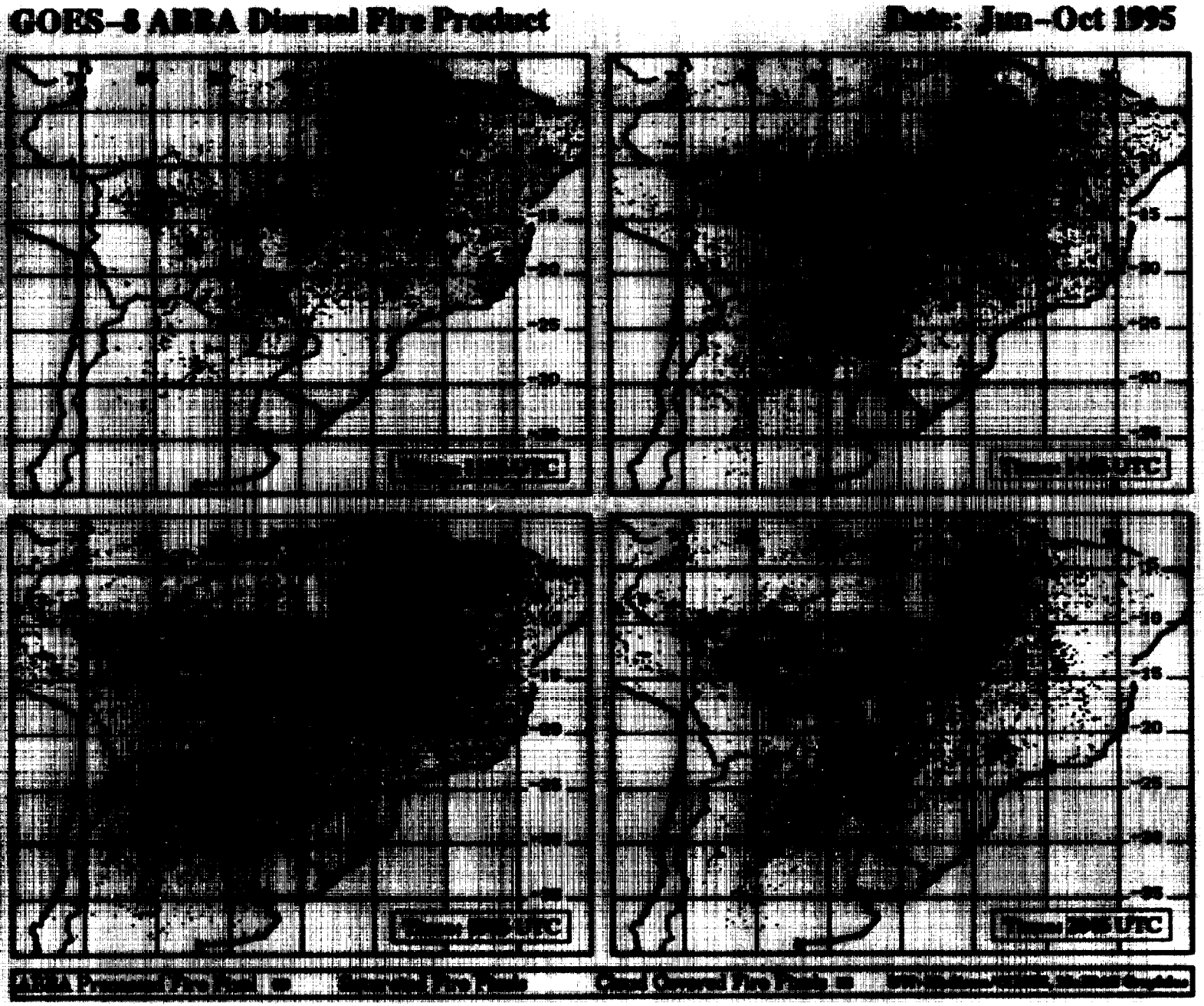

Figure 7. This composite shows the locations of all GOES-8 ABBA detected fire pixels at 1145, 1445, 1745 and 2045 UTC during the 1995 fire season in South America. Burning along rivers and in areas with recent road construction and associated settlements within Amazonia are most evident at 1745 UTC.

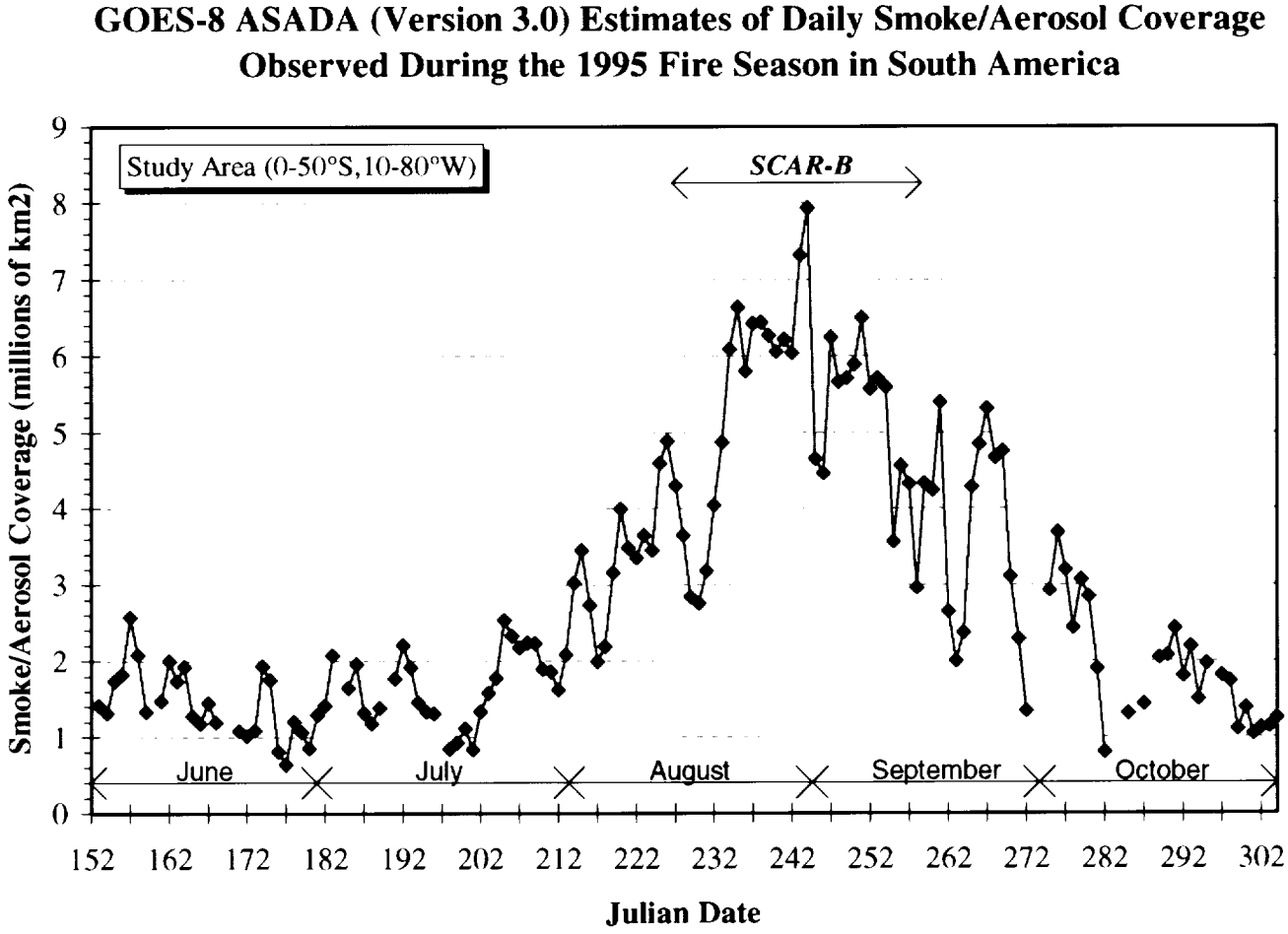

Figure 8. GOES-8 ASADA estimates of daily (at 11:45 UTC) smoke/aerosol coverage during the 1995 fire season in South America.